

# Fluid–solid coupling numerical simulation of charge process in variable-mass thermodynamic system

HU Ji-min(胡继敏), JIN Jia-shan(金家善), YAN Zhi-teng(严志腾)

College of Naval Architecture and Power Engineering, Naval University of Engineering, Wuhan 430033, China

© Central South University Press and Springer-Verlag Berlin Heidelberg 2012

**Abstract:** A joint solution model of variable-mass flow in two-phase region and fluid–solid coupling heat transfer, concerned about the charge process of variable-mass thermodynamic system, is built up and calculated by the finite element method (FEM). The results are basically consistent with relative experimental data. The calculated average heat transfer coefficient reaches  $1.7 \times 10^5 \text{ W}/(\text{m}^2 \cdot \text{K})$ . When the equal percentage valve is used, the system needs the minimum requirements of valve control, but brings the highest construction cost. With the decrease of initial steam pressure, the heat transfer intensity also weakens but the steam flow increases. With the initial water filling coefficient increasing or the temperature of steam supply decreasing, the amount of accumulative steam flow increases with the growth of steam pressure. When the pressure of steam supply drops, the steam flow gradient increases during the maximum opening period of control valve, and causes the maximum steam flow to increase.

**Key words:** steam accumulator; variable-mass; control valve; fluid–solid coupling; numerical simulation

## 1 Introduction

The variable-mass thermodynamic system, which is critical for converting the ability of lower steam supply to higher steam supply, consists of superheated steam source, steam accumulator, charge control valve and the steam pipes connecting them. The steam accumulator offers the steam of required pressure and quantity for instantaneous consumption of steam users in an extremely short time, whose storage mode is similar to the conventional industrial steam accumulator [1–2]. The instant charge process in the system, which is related to the variable-mass flow in two-phase region, fluid-solid coupling heat transfer of steam accumulator, the variable flow resistance characteristics of steam pipes and the dynamical matching problems between the steam accumulator and control valve, is quite different from the objects studied in Refs. [3–6]. So, there are no relevant reports on this research yet.

Based on the charge process of the system [7–8], a joint solution model is built up for calculating the dynamic characteristics of system and the temperature distribution of steam accumulator wall. Moreover, the influences of control valve selection, the initial steam pressure, the initial water filling coefficient and the steam supply parameters on the flow and heat transfer

characteristics of system are also discussed, which provides a theoretical support for system optimal design.

## 2 Object overview

The basic components of the system are shown in Fig. 1. The steam accumulator is a pressure vessel storing hot water and steam for heat release. The lower part of the steam accumulator is a liquid space and the upper part is a vapor space. At runtime, the superheated steam in steam pipes is sprayed from steam source into the liquid space through the control valve. After mixing with the liquid water, the water cycle is formed by the double impacts of the steam jet momentum and the pressure difference inside and outside, then the wet steam is heated to the required pressure and temperature.

Under the conditions of same steam supply parameters, the steam flow depends on two factors: one is the opening of control valve, and the greater the opening, the higher the steam flow. The other is the back pressure of control valve (steam pressure in the steam accumulator), and the higher the steam pressure, the smaller the steam flow. But the steam pressure increases at the steam filling. Therefore, the change rule of steam flow is obtained based on qualitative analysis. At the beginning, the relatively lower steam pressure leads to a larger pressure difference of control valve. With the

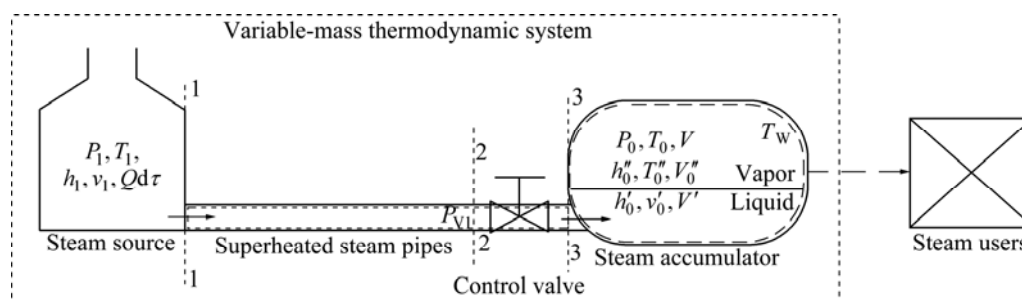


**Fig. 1** Basic structure of variable-mass thermodynamic system

increase of valve opening, the steam flow increases rapidly. On the one hand, the increase of pipes resistance decreases the inlet pressure of control valve, while the steam pressure of steam accumulator also gradually increases. When the valve opening reaches the maximum value, the increase of steam pressure gradually causes the decrease of the steam flow. In the final stage, the steam flow sharply declines due to the joint decrease of the opening and the pressure difference of control valve.

The above qualitative analysis is also confirmed by the experimental data from relevant work [6]. For truly reflecting the wall temperature distribution of a steam accumulator during the charge process, the temperature measurement experiment was carried out [6]. The temperature measurement system consists of steam accumulator, thermocouples, single-chip microcomputer, system machines and glass thermometer. The 48 calibrated thermocouples were respectively installed on the axial and circumferential directions of the steam accumulator wall, and 16 were respectively installed on the inner and outer surface of steam accumulator wall and in the environment. In the experiment, thermoelectric power data from the thermocouples are collected by single-chip microcomputer and then converted to wall temperature data during the charge process of steam accumulator. The large amounts of temperature data obtained show that the wall temperature changes obviously with rules by system machines during the charge process. In most of the charge time, the wall temperature changes linearly with time, while there is a difference only in the initial and final states of the charge process.

In conclusion, as the request of completing charge process within a short time and reaching a required steam pressure in the steam accumulator, the common closed-loop control [9–11] is difficult for the system process control. The research of open-loop process control needs the thermodynamic process model for system.

In addition, the heat transfer of natural convection and steam condensation are also conducted on the steam accumulator wall, which respectively contact with the

liquid space and vapor space, during the entire charge process. Relevant experiments [6] have shown that the temperature distribution of each point on the steam accumulator wall forms certain temperature differences basically according to the vapor space and liquid space. That is to say, the wall contacting with the upper vapor space is heated up much faster, while the temperature change of the wall contacting with the lower liquid space is not obvious. According to the above analysis, if neglecting the heat transfer all above, especially the latter of dramatic phase changes, the final steam pressure of steam accumulator will result in value deviation through the control valve. Moreover, the thermal stress, caused by uneven temperature distribution of the wall, brings certain impacts on the safe operation and lifetime of system. Therefore, detailed analysis is necessary for the flow and heat transfer characteristics of charge process in the system.

As for the heat transfer problems between the wet steam and the metal wall in steam accumulator, the thermal boundary conditions, including steam temperature and heat transfer coefficient, are parts of calculation results, rather than the known conditions, due to the constraining relationship between the flow and metal wall. Above problems bring some difficulties for the numerical study. A better method of solving the problem is combining the thermodynamic process model and the temperature field calculation model, and then calculating the fluid–solid coupling heat transfer under the open-loop control strategy.

The key of the calculation of fluid–solid coupling heat transfer is the implementation of heat transfer between the wet steam and metal wall which can be described by the Fourier heat conduction equation and the control equations [12–13]. The calculation procedure is shown in Fig. 2. Calculated by the thermodynamic process model, the steam temperature and heat transfer coefficient are mapped to the finite element mesh, and integrated into the third type of thermal boundary conditions according to the format of finite element method (FEM) boundary. The boundary condition is then passed to temperature field calculation model using

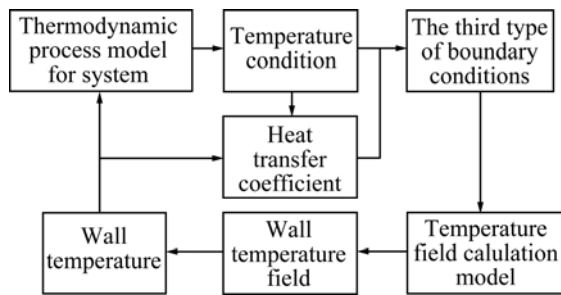


Fig. 2 Calculating flowchart of fluid-solid coupling

MATLAB software. In the end, the wall temperature is calculated using iterative method, which begins with the third condition and continues until the wall temperature converges.

### 3 Calculation model

In Fig. 1,  $\tau$  is the time variable;  $P_1$ ,  $T_1$ ,  $h_1$  and  $v_1$  are respectively the constant superheated steam pressure (MPa), temperature ( $^{\circ}\text{C}$ ), specific enthalpy (kJ/kg) and specific volume ( $\text{m}^3/\text{kg}$ ) at cross-section 1–1 from the exit of steam source;  $Q$  is the instantaneous charge steam flow (kg/s);  $P_{V1}$  is the inlet pressure of control valve (MPa) at cross-section 2–2;  $P_0$  and  $T_0$  are respectively the wet steam pressure and temperature of steam accumulator at cross-section 3–3;  $h_0$ ,  $v_0$ ,  $V$  and  $a$  are respectively the enthalpy, specific volume, volume and water filling coefficient of working fluid in steam accumulator;  $T_w$  is the average temperature of steam accumulator internal wall; superscript “'” and “''” represent the liquid and vapor space parameters of wet steam, respectively.

According to the basic working principle of system, a mathematical model is established in the allowed scope and following assumptions: each component is connected in series at the level of system; the potential energy and kinetic energy of working fluid and the steam leakage during charge process are ignored. Control valve operates without delay, the connect pipes are round diameter, and the superheated steam in the pipes is assumed to be incompressible fluid. Steam accumulator is a rigid storage vessel, of which the internal parameters are treated as lumped parameters. The heat transfer between the outside wall of steam accumulator and the environment can be neglected due to the thick thermal insulation layer. Based on the above assumptions, the model of the system is established by applying theories of variable-mass thermodynamics, viscous fluid mechanics and FEM.

#### 3.1 Thermodynamic model for steam accumulator working process

Adopting the space in steam accumulator as a

control volume for thermodynamic analysis, the state change rule of the working fluid in the control volume simultaneously satisfied the conservation equations of mass, energy and volume [7].

No mass flows out of the control volume during the charge process ( $\sigma m=0$ ). With the continuous differential equations [14], the instantaneous superheated steam flows are all  $Q$  both at the pipe cross-sections 1–1 and 3–3 (see Fig. 1), so the working fluid in the control volume satisfies the mass conservation equation as

$$Qd\tau = d(V'/v'_0 + V''/v''_0) \quad (1)$$

Although frictional resistance of steam flow in the process is irreversible for a part of the mechanical energy is changed into heat, the instantaneous energies of superheated steam at cross-sections 1–1 and 3–3 are all  $h_1 \cdot Q$  if ignoring the potential energy changes and heat exchange with the environment. Therefore, the working fluid in the control volume satisfies the energy conservation equation as

$$[h_1 \cdot Q - \alpha A(T_0 - T_w)/1000]d\tau = d(u'_0 V'/v'_0 + u''_0 V''/v''_0) \quad (2)$$

where  $u_0$  is the specific internal energy of working fluid (kJ/kg);  $\alpha$  and  $A$  are respectively the heat transfer coefficient and the surface area in steam accumulator;  $\alpha$  and  $T_w$  are obtained from the calculation of fluid–solid coupling heat transfer model;  $\Delta T$  is defined as the average temperature difference ( $\Delta T = T_0 - T_w$ ).

At the same time, the working fluid in the control volume also satisfies the volume conservation equation by

$$V = V' + V'' = V' \alpha = C \quad (3)$$

According to the thermodynamic property of water and steam, the characteristic parameters of superheated steam are determined by the temperature and pressure. While the characteristic parameters in liquid/vapor space of wet steam are only a single-valued function of pressure or temperature, which can be calculated by the International Association for the Properties of Water and Steam (IAPWS) for the thermodynamic properties of water and steam [8]:

$$h_1 = h_1(P_1, T_1), v_1 = v_1(P_1, T_1) \quad (4)$$

$$v'_0 = v'_0(P_0), h'_0 = h'_0(P_0), u'_0 = h'_0 - P_0 \cdot v'_0 \quad (5)$$

$$v''_0 = v''_0(P_0), h''_0 = h''_0(P_0), u''_0 = h''_0 - P_0 \cdot v''_0 \quad (6)$$

According to Eqs. (1)–(6), there is a reciprocal one-to-one correspondence between the steam pressure and the accumulative steam flow in steam accumulator.

#### 3.2 Flow dynamics model for superheated steam in steam pipes

During the charge process by control valve, the

superheated steam flow adiabatics in the pipes under the effect of pressure difference between the steam source and steam accumulator, leads to the existence of frictional drag and various kinds of local resistance. To facilitate the calculation, the local resistance caused by pipe joints, corners and other components can be converted into the equivalent length and then can be calculated together with the total length  $L$  of resistance.

Due to the superheated steam flows in pipes keeping at turbulent flowing section, its resistance drag coefficient  $\lambda$  can be obtained by the iterative calculations of Colebrook equation [14]:

$$\frac{1}{\sqrt{\lambda}} = 2 \lg \left( \frac{k/D}{3.7} + \frac{2.51}{Re\sqrt{\lambda}} \right) \quad (7)$$

where  $Re$  is Reynolds number,  $D$  is the inner diameter of steam pipes, and  $k$  is the pipes equivalent roughness.

And then pressure drop  $\Delta P_p$  is calculated by Darcy's formula:

$$\Delta P_p = P_1 - P_{V1} = \frac{\lambda L}{2000D} \cdot \frac{v_1(P_1, T_1) \cdot Q^2}{S^2} \quad (8)$$

### 3.3 Flow characteristics model for control valve

Many studies on the ideal and work flow characteristics of control valve are conducted under the condition of constant system pressure difference. While in the system, the steam pressure determined by the accumulative steam flow varies with the charge time, the pressure difference of system is no longer constant. Therefore, the relevant achievements of above studies cannot be directly applied, which needs the derivation of applicable mathematical model for flow characteristics.

There are mainly three kinds of flow characteristics about control valve: equal percentage, linear and quick opening. Among them, the relative valve opening is proportional to the relative steam flow of logarithm under the pressure difference  $\Delta P_V$  of the control valve at the flow characteristics of equal percentage [10–11]:

$$Q/Q_{\max} = (Q_{\max}/Q_{\min})^{l/L-1} \quad (9)$$

where  $l/L$  is the relative valve opening,  $Q_{\max}$  and  $Q_{\min}$  respectively refer to the steam flow under pressure difference  $\Delta P_V$  of control valve, when the control valve is at maximum and minimum of the relative opening. Without the blocked flow in charge process,  $Q_{\max}$  and  $Q_{\min}$  are calculated by

$$Q_{\max(\min)} = 20\sqrt{5}S\sqrt{\Delta P_p \cdot \rho} / \sqrt{\xi_{\min(\max)}} \quad (10)$$

where  $\xi_{\min}$  and  $\xi_{\max}$  respectively correspond to the resistance coefficient of  $Q_{\max}$  and  $Q_{\min}$ , only related to the shape and opening of control valve. So, they are all constants under the conditions of any pressure difference. Putting Eq. (10) into Eq. (9), there is

$$\sqrt{\xi_{\min}} / \sqrt{\xi} = (\sqrt{\xi_{\max}} / \sqrt{\xi_{\min}})^{l/L-1} \quad (11)$$

Further, integrate the Eq. (11) into the flow equation of control valve,

$$Q = C_1^{1/L} C_2 \sqrt{\Delta P_V \cdot \rho} \quad (12)$$

where  $C_1 = \sqrt{\xi_{\max}} / \sqrt{\xi_{\min}}$  and  $C_2 = 20\sqrt{5}S / \sqrt{\xi_{\max}}$ . It is observed that  $C_1$  and  $C_2$  are both constants when the valve type is chosen, while steam flow varies with  $l/L$  and  $\Delta P_V$ . For a pressure difference  $\Delta P_V$  of the valve, there are

$$C_2 = Q_{\min} / \sqrt{\Delta P_V \cdot \rho}, \text{ when } l/L = 0 \quad (13)$$

$$C_1 C_2 = Q_{\max} / \sqrt{\Delta P_V \cdot \rho}, \text{ when } l/L = 1 \quad (14)$$

Based on the definition of ideal range ability  $R$  in control valve, Eq. (12) is divided by Eq. (13):

$$C_1 = Q_{\max}/Q_{\min} = R \quad (15)$$

Similarly, the mathematical model of linear valve and quick opening valve can also be derived by the above-mentioned method. Thus, a joint model expressed by Eqs. (1)–(15) is the thermodynamic process model for system.

### 3.4 Temperature field calculation model of steam accumulator wall

Due to the fact that the steam accumulator is a thin-walled cylinder (see Fig. 3), and the  $L/D$  ratio is relatively large, the temperature field calculation model is simplified to an unsteady heat conduction problem of two-dimensional wall with constant properties, isotropic and no internal heat source, which satisfies the parabolic partial differential equation:

$$\left[ \frac{\partial}{\partial x} \left( \lambda \frac{\partial T_w}{\partial x} \right) + \frac{\partial}{\partial y} \left( \lambda \frac{\partial T_w}{\partial y} \right) + \frac{\partial}{\partial z} \left( \lambda \frac{\partial T_w}{\partial z} \right) \right] = \rho c \frac{\partial T_w}{\partial t} \quad (16)$$

where  $\rho$  is the wall density of metal ( $\text{kg/m}^3$ ),  $\lambda$  is the

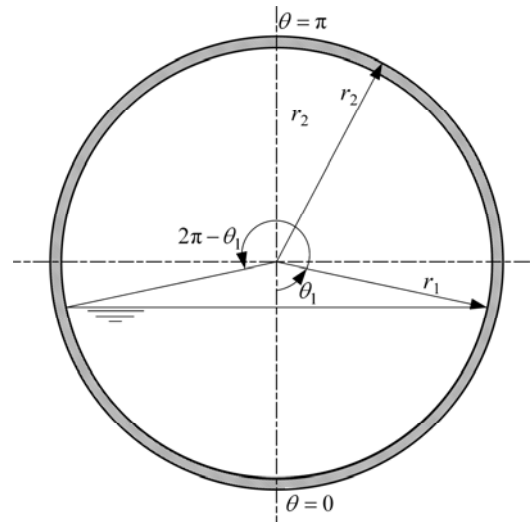


Fig. 3 Cross section structure of steam accumulator

thermal conductivity of metal wall ( $\text{W}/(\text{m} \cdot \text{K})$ ), and  $c$  is the heat capacity of metal wall ( $\text{J}/(\text{kg} \cdot \text{K})$ ).

Because the environmental conditions of the wall can be regarded as adiabatics, the heat transfer of natural convection and steam condensation, respectively, occurring in liquid-wall space and vapor-wall space, are the third type of boundary conditions in the charge process.

The wall temperature is assumed to be uniform at the beginning of charge process, that is, the initial boundary temperature (steam temperature). The time curve of steam temperature is calculated by the thermodynamic process model for system:

$$t=0, 0 \leq \theta \leq 2\pi \Rightarrow T=T_0 \quad (17)$$

During the charge process, the heat transfer occurring between the wall and steam is linear with Neumann boundary conditions:

$$t=0, 0 \leq \theta \leq 2\pi \Rightarrow -\lambda \cdot (\partial T / \partial n) = \alpha(T_f - T_w) \quad (18)$$

where  $r_1$  is the inner diameter of the wall.

The convection heat transfer coefficient is divided into steam condensation of the upper part  $\alpha_1$  and natural convection of the lower part  $\alpha_2$  for steam accumulator:

$$\alpha = \begin{cases} \alpha_1, \theta_1 \leq \theta \leq 2\pi - \theta_1 \\ \alpha_2, -\theta_1 \leq \theta \leq \theta_1 \end{cases} \quad (19)$$

where  $\alpha_2$  can be chosen as a constant in the range of  $200\text{--}1\,000 \text{ W}/(\text{m}^2 \cdot \text{K})$ , while the steam condensation heat transfer coefficient  $\alpha_1$  much larger than the former, which ranges from  $5 \times 10^3$  to  $2.5 \times 10^4 \text{ W}/(\text{m}^2 \cdot \text{K})$ , can be calculated by [15]

$$\alpha_1 = 1.13 \left[ \frac{g r_s \rho_s^2 \lambda_s^3}{2 \eta_s r_1 (T_0 - T_w)} \right]^{1/4} \quad (14)$$

where  $r_s$  is the latent heat of vapor steam, which can be calculated by the IAPWS for the thermodynamic properties of water and steam,  $g$  is the acceleration of gravity, taken as  $9.8 \text{ m/s}^2$ . The unknown parameters of  $T_0$  and  $T_w$  are respectively calculated by thermodynamic process model and temperature field calculation model. Other property parameters, including water film density  $\rho_s$ , thermal conductivity coefficient  $\lambda_s$  and dynamic viscosity  $\eta_s$ , are calculated according to the average temperature  $T_m = (T_0 + T_w)/2$  of water film.

The adiabatic outside is also linear with Neumann boundary conditions:

$$r=r_2, 0 \leq \theta \leq 2\pi \Rightarrow -\lambda \cdot (\partial T / \partial n)_w = 0 \Rightarrow (\partial T / \partial n) = 0 \quad (21)$$

where  $r_2$  is the outer diameter of the wall. After the temperature field of two-dimensional wall is modeled, it can be numerically calculated by FEM, combined with the calculation of thermodynamic process model. Finally,

the time curves of wet steam and wall temperature during the charge process can be obtained.

Thus, the combination equations obtained by the above sections is a joint solution model of variable-mass flow in two-phase region and fluid–solid coupling heat transfer, concerning about the charge process of the system. The mathematical model can be calculated when the conditions of valve control strategy, steam supply parameters, initial steam pressure, initial water filling coefficient, wall structure and property parameters, and characteristic parameters of pipes and control valve are given. It can be seen that, although the analytical solutions are hardly obtained by the above model for the complexity, the numerical simulation methods can be applied to relevant studies for solving problem.

## 4 Numerical simulation and results analysis

### 4.1 Temperature field analysis of steam accumulator wall

The temperature field calculation model of steam accumulator wall is calculated by MATLAB/Pdtool of two-dimensional finite element solver for geometric modeling, boundary condition setting, equation type determining, triangle mesh partitioning, and equation solving. Figure 4 shows the FEM model of steam accumulator wall.

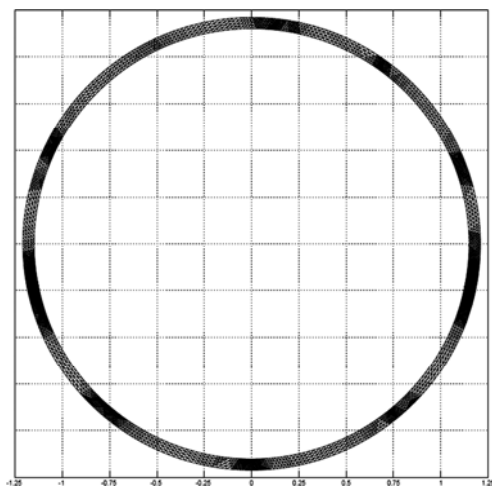


Fig. 4 FEA model of steam accumulator wall

Among them, the average heat transfer coefficient is initially determined by a given value with the boundary condition setting, while the time curve of boundary steam temperature is obtained from the thermodynamic process model with neglecting the heat transfer.

In Fig. 4, the calculation area consists of two parts, which respectively contact with the upper vapor space and the lower liquid space of metal wall. A further mesh refinement of the computational domain, with the total number of 16 448 grids, brings the accurate simulation of

heat transfer characteristics after the mesh partition. The main parameters used for the model are listed in Table 1.

**Table 1** Main parameters used for model

Parameter	Value
Density, $\rho/(\text{kg}\cdot\text{m}^{-3})$	7 830
Heat capacity, $c/(\text{J}\cdot\text{kg}^{-1}\cdot\text{K}^{-1})$	460
Thermal conductivity, $\lambda/(\text{W}\cdot\text{m}^{-1}\cdot\text{K}^{-1})$	25
Inner radius, $r_1/\text{m}$	1.13
Length, $L_1/\text{m}$	8.8
Initial water filling coefficient, $a/\%$	30

## 4.2 Simulation of thermodynamic process model for system

The simulation modules of each subsystem unit in the thermodynamic process model are created and connected by MATLAB/Simulink [16]. Figure 5 shows the simulation block diagram which contains the encapsulated subsystem unit of steam accumulator, control valve, pipes, thermodynamic property of water and steam and control strategy. The subsystem unit of steam accumulator (CQT\_unit), specified by giving the steam pressure and the accumulative steam flow in steam accumulator, is the core of thermodynamic process model for system. The subsystem unit of control strategy (I\_valve) is used for the control valve with control strategy of action time. The subsystem unit of control

valve and pipes (valve\_unit) is used for calculating the steam flow and pipes resistance with three kinds of flow characteristics about control valve: equal percentage, linear and quick opening. The IAPWS [8] is applied to the subsystem unit of thermodynamic property of water and steam, so the steam pressure of steam accumulator is the only input in the subsystem. The wall temperature of steam accumulator unit is provided by the temperature field calculation model.

## 4.3 Results analysis of joint solution model

The joint solution model consists of temperature field calculation model and thermodynamic process model is numerically simulated with the main parameters (respectively listed in Table 1 and Fig. 5), and the valve control strategy of action time parameter (see Fig. 6) are given. The steam user requirement of completing steam charge process should be within 45 s and the required pressure of 5.6 MPa is reached.

Figure 7 shows the numerical simulation results of flow and heat transfer characteristics during the charge process. Figure 7(a) shows that the change of the steam flow with the equal percentage valve is the slowest during opening at the beginning and closing in the end, followed by the linear valve, and the most intense is the quick opening valve. Therefore, when the equal percentage valve is used, the system needs the minimum requirements of valve control, but needs the maximum

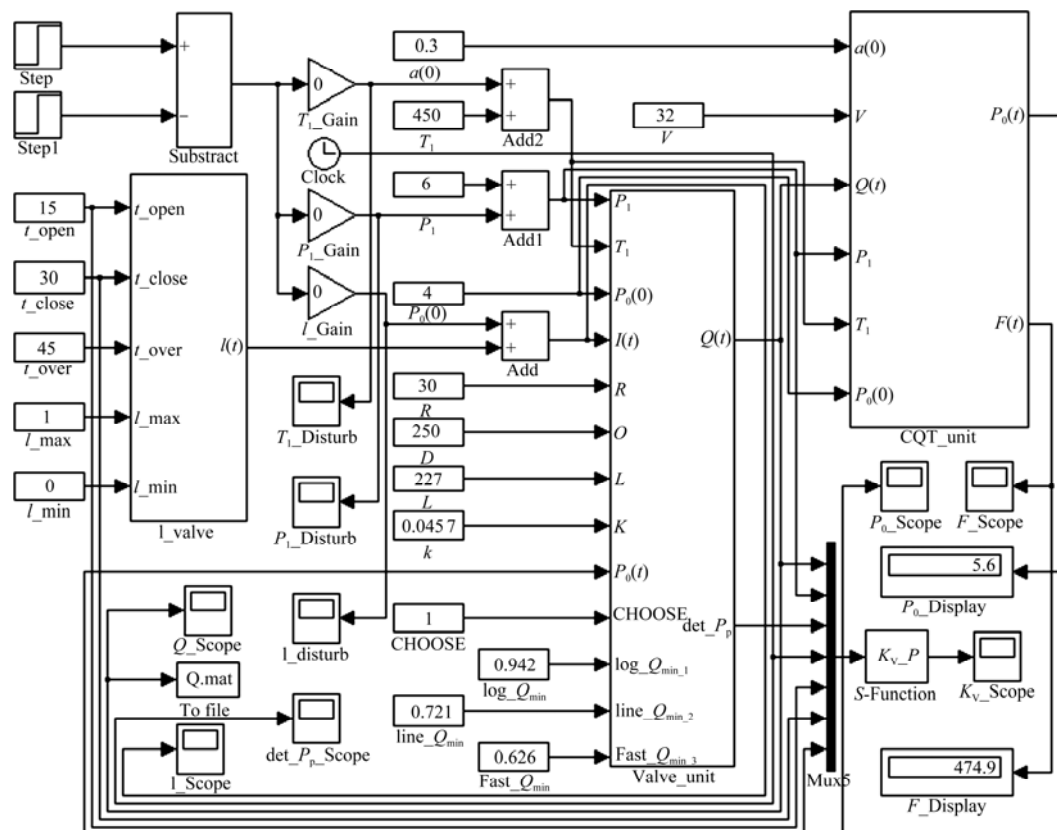


**Fig. 5** System model

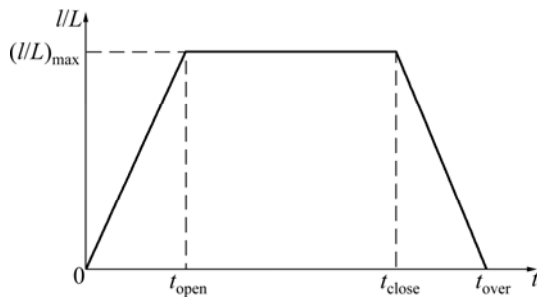


Fig. 6 Action time parameter of control valve

diameter, which brings the highest construction costs and steam supply of steam source. All the points deserve to be weighed for the system design considerations. For the equal percentage valve, the max steam flow  $Q_{\max}$  is 24.9 kg/s, followed by linear valve, which is 18.4 kg/s, and the smallest value is 15.9 kg/s of quick opening valve. In addition, the steam flows of three types of control valve all experience a similarly linear decline process during the maximum opening of control valve. Figure 7(b) shows the variable trend of the steam pressure. It is consistent with the accumulative steam flow, determined by the reciprocal one-to-one correspondence between both of them from Eqs. (1) to (6). From Fig. 7(c), it is obtained that the highest temperature

reaches 269.1 °C, occurring at the upper wall in contact with vapor space, and gradually decreases with the heat spreading out. The temperature of the lower wall in contact with liquid space doesn't change (250.4 °C), while it drops by 18.7 °C for the upper wall. The results are consistent with the experimental data that the heat transfer intensity of steam condensation is much greater than that of water natural convection, and the average heat transfer coefficient reaches  $1.7 \times 10^4 \text{ W}/(\text{m}^2 \cdot \text{K})$ . The temperature curves of wet steam ( $T_{00}$  and  $T_0$ ) and metal wall ( $T_W$ ) are shown in Fig. 7(d), where, the heat transfer is considered for the curves of  $T_0$  and  $T_W$  but not for the curve of  $T_{00}$ . It can be seen that, as  $T_0$  rises,  $T_W$  also rises, but the variation trend of  $T_W$  significantly lags behind  $T_0$ . The temperature trend of  $T_{00}$  and  $T_0$  is basically consistent with each other, but the rise trend of  $T_0$  is slower than  $T_{00}$ , and an obvious difference occurs especially in the end of charge process. This indicates that the heat transfer of steam condensation accounts for certain proportion in energy charge process. At the same time, the steam pressure without considering the heat transfer increases by 1.6 MPa (the corresponding temperature increases from 250.4 °C to 271.1 °C), while the latter with considering the heat transfer (the corresponding temperature increases from 250.4 °C to

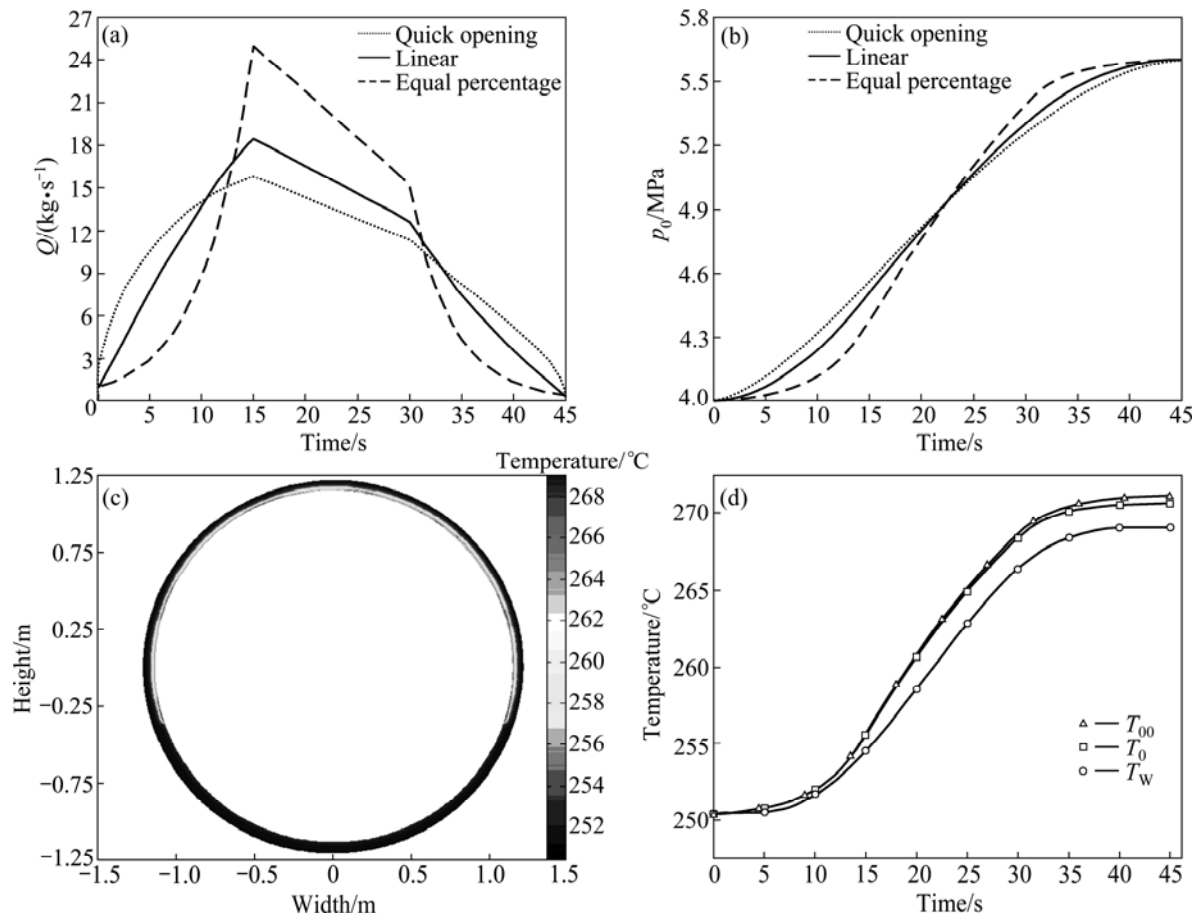


Fig. 7 Simulation results: (a) Steam flow during charge; (b) Wet steam pressure during charge; (c) Temperature distribution of steam accumulator wall; (d) Temperature of wet steam and wall during charge

270.3 °C) is 4.4% less than the former. The above results illustrate that the former is more accordant with the actual conditions than the latter.

## 5 Analysis on influencing factors

### 5.1 Influence of initial steam pressure on flow and heat transfer characteristics

Figure 8 shows the steam flow curves of the system by valve control strategy when the initial wet steam pressures are 5.0, 4.5, 4.0 and 3.5 MPa, respectively. As the initial steam pressure decreases, the steam accumulator must be charged with greater amount of steam and achieve the steam user requirements for system, which leads to the joint increase of the gradient and maximum ( $Q_{\max}$ ) of steam flow, and the values of  $Q_{\max}$  reach 8.1, 16.1, 24.9 and 34.6 kg/s, respectively.

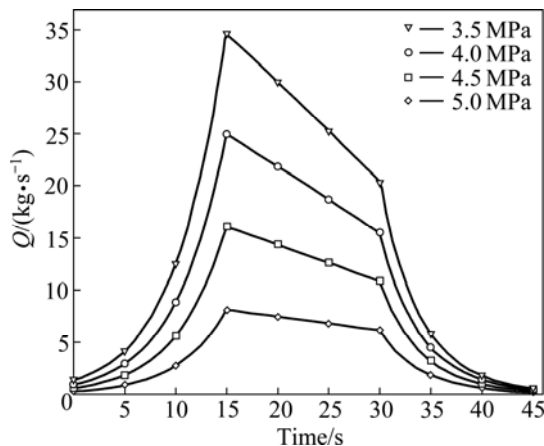


**Fig. 8** Time curves of steam flow under different initial wet steam pressures

Figure 9 shows the time curves of wet steam  $T_0$  and wall temperature  $T_w$  under the different initial wet steam pressures. When the initial wet pressure  $P_0$  is 5.0 MPa, both the temperature gradient and temperature difference  $\Delta T$  of heat transfer are relatively smaller, while the average film temperature  $T_m$  is relatively larger, thus leading to a relatively higher value of condensation heat transfer coefficient  $\alpha_1$ . As the initial pressure decreases, the temperature gradient increases correspondingly but  $\alpha_1$  gradually decreases, which brings to weakened heat intensity. At the same  $T_0$  in the end of charge process,  $T_w$  is gradually decreases. Temperatures are 270.4, 269.8, 269.1 and 268.3 °C when the initial wet steam pressures are 5.0, 4.5, 4.0 and 3.5 MPa, respectively.

Calculations also demonstrate that, the heat transfer intensity varies with the different initial steam pressures. However, the change rule of the energy proportion of the heat transfer (et\_H) in the charge process is coincident under the joint actions of  $Q$ ,  $h_1$ ,  $\alpha_1$  and  $\Delta T$ .

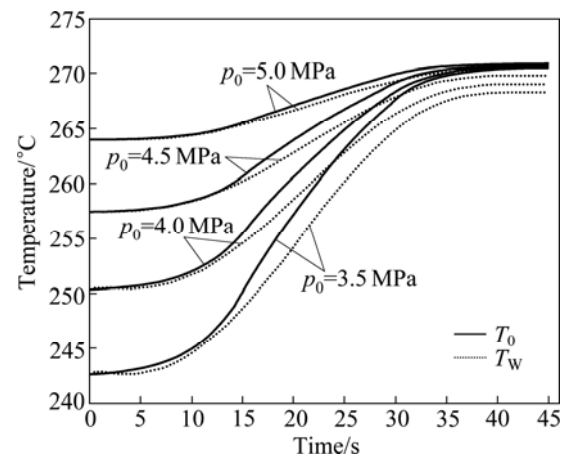


**Fig. 9** Time curves of wet steam and wall temperature under different initial wet steam pressure

### 5.2 Influence of initial water filling coefficient on flow and heat transfer characteristics

Figure 10 shows the time curves of main parameters, including the steam flow  $Q$ , the energy proportion of the heat transfer (et\_H) in charge process, the incremental ratio of water fill coefficient  $\Delta a/a$  and steam pressure  $\Delta P_0/P_0$ , under the conditions of different initial water filling coefficients. As the initial water filling coefficient increases from 30% to 50%, the maximum value of  $Q$  also increases from 24.9 kg/s to 34.9 kg/s. At the same time, the amount of steam flow accumulation increases from 478.9 kg to 674.8 kg, with the growth of 40.9%. However, the change rule of the incremental ratio of steam pressure  $\Delta P_0/P_0$  is coincident, though the initial water filling coefficient changes. It can be explained from Eqs. (1)–(6) that, with the increase of the initial water filling coefficient, the function of the accumulative steam flow and steam pressure also changes simultaneously, which leads to the amount of steam flow accumulation increasing in the same growth of steam pressure. The results indicate that the initial water filling

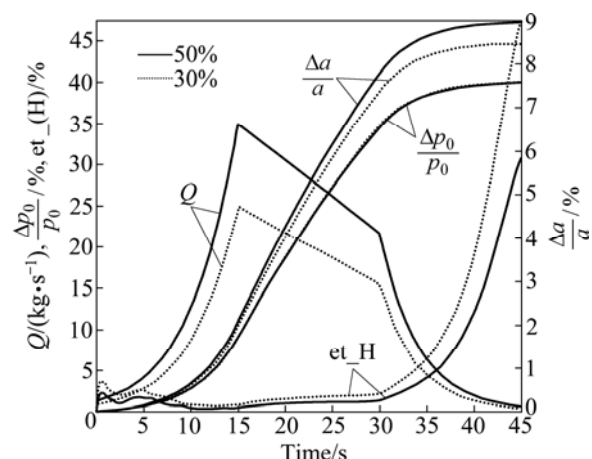


**Fig. 10** Time curves of main parameters under different initial water filling coefficients



coefficient directly affects the accumulative steam flow and finally affects the steam amount of the steam users.

In addition, Fig. 10 shows that, the incremental ratio of water fill coefficient  $\Delta a/a$  (the water level in steam accumulator) gradually increases during the charge process with the initial water filling coefficient increasing. When the initial water fill coefficient is 30% and 50%, the maximum value of  $\Delta a/a$  are 8.47% and 8.96% respectively. On the contrary, the growth of  $et_H$  slows down with the initial water filling coefficient increasing. When the initial water fill coefficient is 30% and 50%, the maximum values of  $et_H$  are 47.7% and 30.5% respectively. Figure 11 shows the wall temperature distribution when the initial water filling coefficient is 50%. The wall temperature distribution and the intensity of heat transfer can almost not be affected, while the  $et_H$  decreases under the joint action of condensation surface area reducing and accumulative steam flow increasing.

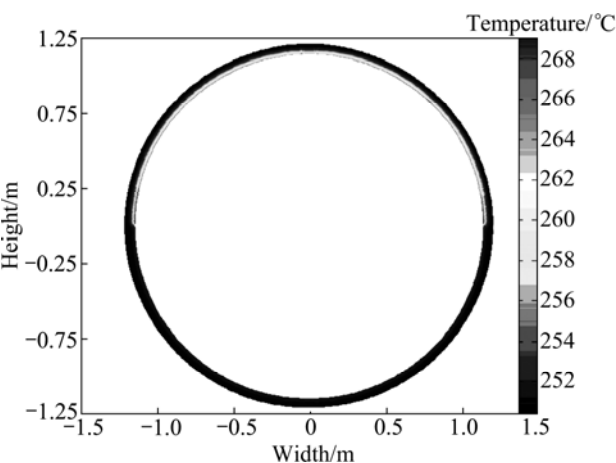


**Fig. 11** Temperature distribution of steam accumulator wall when initial water filling coefficient of 50%

### 5.3 Influence of steam supply parameters on flow and heat transfer characteristics

Numerical calculations show that, only analyzing the influence of supply parameters on the flow characteristics is appropriate, because of the little effect on the heat transfer characteristics. Figure 12 shows the time curves of the main parameters with different steam supply parameters, including the steam flow  $Q$ , the incremental ratio of water fill coefficient  $\Delta a/a$  and the steam pressure  $\Delta P_0/P_0$ . As the temperature of steam supply decreases,  $Q_{\max}$ , the growth velocity and the maximum value of  $\Delta a/a$  all increase, while the change rule of the steam flows gradient and  $\Delta P_0/P_0$  remains unchange during the maximum opening period maintained by the control valve. As the pressure of steam supply drops,  $Q_{\max}$  and the steam flow gradient both increase, while  $\Delta a/a$  and  $\Delta P_0/P_0$  slightly increase in the middle period (10–35 s), but there is no change in the

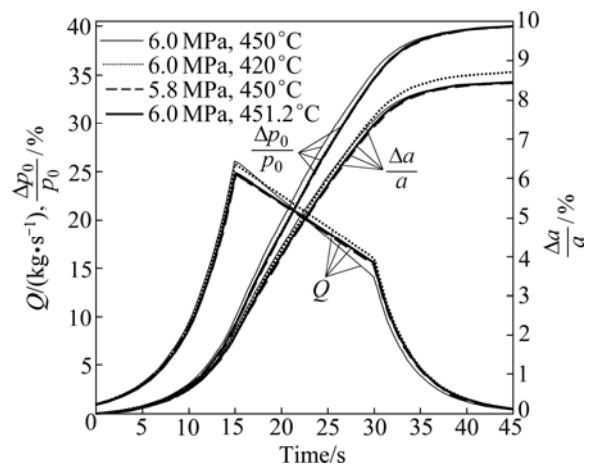


**Fig. 12** Time curves of main parameters under different steam supply parameters

end of charge process (35–45 s).

It can be obtained from Table 2 that, as the temperature of steam supply decreases, the amount of accumulative steam flow increases to meet the requirements from steam users, with a rise of about 0.58 kg/°C. As the pressure of steam supply drops, the amount of accumulative steam flow also decreases with a drop of 0.3 kg/MPa, due to the increase of specific enthalpy.

Figure 12 and Table 2 also show the variation characteristics of main parameters when changing the temperature (6.0 MPa, 451.2 °C) and the pressure (5.8 MPa, 450 °C) of steam supply, respectively, at the same specific enthalpy (3 305.6 kJ/kg). The maximum steam flows  $Q_{\max}$  are 24.8 kg/s and 26.2 kg/s, and the amounts of steam flow accumulation are 478.0 kg and 478.3 kg respectively. Therefore, the main differences are the steam flow gradient and  $Q_{\max}$ . Moreover, the change rule of  $\Delta P_0/P_0$  remains unchange under the

**Table 2** Calculated values of steam flow accumulation under different steam supply parameters

Pressure/ MPa	Temperature/ °C	Specific enthalpy/ (kJ·kg <sup>-1</sup> )	Flow accumulation/kg
6.0	451.2	3 305.6	478.0
6.0	450.0	3 302.8	478.9
6.0	440.0	3 228.8	484.3
6.0	430.0	3 253.7	490.1
6.0	420.0	3 228.8	495.9
6.0	410.0	3 203.6	501.9
6.0	400.0	3 178.2	507.5
5.9	450.0	3 304.2	478.6
5.8	450.0	3 305.6	478.3
5.7	450.0	3 307.1	478.0

different temperatures of steam supply, while the accumulative steam flow changes, and the function of steam flow accumulation and steam pressure change simultaneously.

## 6 Conclusions

1) The dynamic characteristic and wall temperature distribution of steam accumulator are numerically simulated by the joint solution model for the charge process in a variable-mass thermodynamic system. The results under consideration of fluid–solid coupling heat transfer are consistent with the distribution of relative experimental data. When the equal percentage valve is used, the system needs the minimum requirements of valve control, and the maximum diameter of control valve, which brings the highest construction costs and steam supply of steam source. All above mentioned effects need to be balanced in the system optimal design.

2) The accumulative steam flow increases with the decrease of the initial steam pressure, which brings the increase of the maximum steam flow and valve diameter, and weakens the heat intensity.

3) With the initial water filling coefficient of steam accumulator increasing or the temperature of steam supply decreasing, the amount of accumulative steam flow increases under the same increase of steam pressure. Moreover, the accumulative steam flow changes and the function of steam flow accumulation and steam pressure change simultaneously.

4) As the steam flow pressure drops, the steam flow gradient increases during the maximum opening period maintained by control valve, leading to the increase of the maximum steam flow and valve diameter.

## References

- [1] CHENG Zu-yu. The application and design of steam accumulator [M]. Beijing: China Machine Press, 1985: 165–168. (in Chinese)
- [2] STEINMANN W D, ECK M. Buffer storage for direct steam generation [J]. *Solar Energy*, 2006, 80(10): 1277–1282.
- [3] BALDINI A, MANFRIDA G, TEMPESTI D. Model of a solar collector/storage system for industrial thermal applications [J]. *Int Centre for Applied Thermodynamics*, 2009, 12(2): 83–88.
- [4] GIL A, MEDRANO M, MARTORELL I, et al. State of the art on high-temperature thermal energy storage for power generation. Part 1: Concepts, materials and modellization [J]. *Renewable and Sustainable Energy Reviews*, 2010, 14: 31–55.
- [5] MEDRANO M, GIL A, MARTORELL I, POTAU X, CABEZA L F. State of the art on high-temperature thermal energy storage for power generation. Part 2: Case studies [J]. *Renewable and Sustainable Energy Reviews*, 2010, 14(1): 56–72.
- [6] LIU Xiao-hui, GONG Chong-ling, LIU Shun-jun. Experimental study and numerical simulation of unsteady temperature field in the heat accumulator cylinder [J]. *Journal of Wuhan Automotive Polytechnic University*, 1996, 18(4): 79–83. (in Chinese)
- [7] WU Pei-yi, MA Yuan. The application of variable-mass system thermodynamics [M]. Beijing: Higher Education Press, 2001: 1–36. (in Chinese)
- [8] WAGNER W, COOPER J R, DITTMANN A, KIJIMA J, KRETZSCHMAR H J, KRUSE A, MARES R, OGUCHI K, SATO H, STÖKER I, SIENER O, TAKAISHI Y, TANISHITA I, TRÜBENBACH J, WILLKOMMEN T. The IAPWS industrial formulation 1997 for the thermodynamic properties of water and steam [J]. *Journal of Engineering for Gas Turbines and Power*, 2000, 122(1): 150–182.
- [9] WILTON S R. Control valves and process variability [J]. *Instrument Society of America Transactions* 2000, 39(2): 265–271.
- [10] LU Pei-yuan. The practical technique of control valve [M]. Beijing: China Machine Press, 2009: 665–671. (in Chinese)
- [11] WU Guo-xi. Operation and maintenance of control valve [M]. Beijing: Chemical Industry Press, 1999: 101–114. (in Chinese)
- [12] ZHOU Nai-jun, ZHOU Shan-hong, ZHANG Jia-qi, PAN Qing-lin. Numerical simulation of aluminum holding furnace with fluid-solid coupled heat transfer [J]. *Journal of Central South University of Technology*, 2010, 17(6): 1389–1394.
- [13] LUO Qing-guo, LIU Hong-bin, GONG Zheng-bo. Study on the fluid-solid coupled heat transfer of the diesel engine cylinder head [J]. *Acta Armamentarii*, 2008, 29(7): 669–773.
- [14] ZHANG Zi-xiong, DONG Zeng-nan. Viscous fluid mechanics [M]. Beijing: Tsinghua University Press, 2005: 351–374. (in Chinese)
- [15] YANG Shi-ming, TAO Wen-quan. Heat transfer [M]. Version 3. Beijing: Higher Education Press, 1998: 206–215. (in Chinese)
- [16] QI Kun-peng, FENG Li-yan, LENG Xian-yin, TIAN Jiang-ping, LONG Wu-qiang. Simulation of quasi-dimensional model for diesel engine working process [J]. *Journal of Central South University of Technology*, 2010, 17: 868–872.

(Edited by DENG Lü-xiang)